TRANSNAV
http://www.transnav.eu
the International Journal
on Marine Navigation
and Safety of Sea Transportation
Volume 19
Number 4
December 2025
DOI: 10.12716/1001.19.04.25

Modified Cylindrical Antenna Array for Maritime Applications

J. Stępień & L. Kachel
Military University of Technology, Warsaw, Poland

ABSTRACT: The article presents modifications of a cylindrical antenna array dedicated to a communication system in marine ap-plications. The possibilities of spatial filtration were investigated by simulation to obtain low sidelobe levels of the 20 dBc order. The results for different antenna elements were compared in terms of frequency filtration for the broadband ones. The optimal characteristics of the antenna system were determined taking into account the influence of the cross-ing level the each antennas radiation characteristics and the radius of their position.

1 INTRODUCTION

Both in marine [1] and space [2] applications, the requirements for high antenna gains are dictated by the need to limit the transmitter power and large ranges of the communication or navigation system, including 5G [3][5] and systems installed on HAPS platforms [6] and in the ground component. Additionally, the platforms on which such solutions are installed are in motion in at least two axes. For this reason, antenna arrays are used that allow for changing the direction of the main radiation.

Other applications include GPS and alternative systems, where it is important to make the receiver [4] resistant to spoofing (mitigation) by controlling the radiation antenna pattern (CRPA), i.e. using directional beam-steering antennas to perform spatial filtering, i.e. suppressing signals coming from all other directions in the receiver system in relation to the angular range of the useful signal.

In this paper, modifications to the antenna array geometry are proposed to reduce the side-lobe levels and increase the angular range. This is a continuation of previous studies [10], in which The MPM was used to model radio channels in [11][12] and the 3GPP channel model [16] in [14][15]. Due to the numerical complexity of the simulation tests of interference between multiple antenna beams, an analysis of the influence of interference from different directions on a single beam was performed.

The required difference between the levels of the main direction of antenna radiation and the side lobes is obtained by appropriately setting the electrical centers of elements or groups of elements and therefore also by building an appropriate power supply network. A small number of elements, e.g. 3 or 4, allows for a range of about ±30◎. Doubling the number of elements allows for increasing the angular range by half, which is also possible by tilting some elements relative to the others and by using lenses.

In the case of a scenario where it would be necessary to increase the gain of the antenna array using converging lenses, the angular range would be reduced, therefore, for X-band and higher frequencies, while for S-band and lower frequencies, the total number of elements in the array was reduced. The

results of calculations and simulations for different antenna pattern models were compared. The optimized parameters [9] of the antenna array allow for obtaining the expected spatial filtration [7] at a level of typically 17-20dBc, the minimum for multiplexing [8].

2 ANALYSIS OF ANTENNA ARRAY

The calculations were made for the circular array constructed of eight sector antennas ( ), tube or patch, working in the S-band, in one example 3.5 GHz, uniformly spaced around a circle with radius r with a spacing of 45 degrees. The analysis of array aimed at determining the radius for which the antenna array radiation pattern would be close to omnidirectional. Figure 1. presents the structure of the analyzed system, where:

θ – angle of the signal arrival in relation to the reference direction of the antenna system, e.g. relative to the north direction (N),

ψ – angle of the antenna layout $\psi = 2\pi/N$,

$d_1, d_2, \ldots, d_n \ldots, d_N$ – distances of the phase centers of the respective antennas to the tangent wave front in *S* point to the circle with *r* radius.

Analysis of the circular antenna array was conducted under the following assumptions:

- electromagnetic wave reaching the antenna is flat one,
- antennas are uniformly spaced around a circle,
- the reference is the antenna, which determines north direction together with the geometric center of the antenna system (in our case, it is antenna No. 1),
- width of the antenna directivity characteristics do not change in the analyzed frequency band,
- minor lobes were omitted in the analysis.

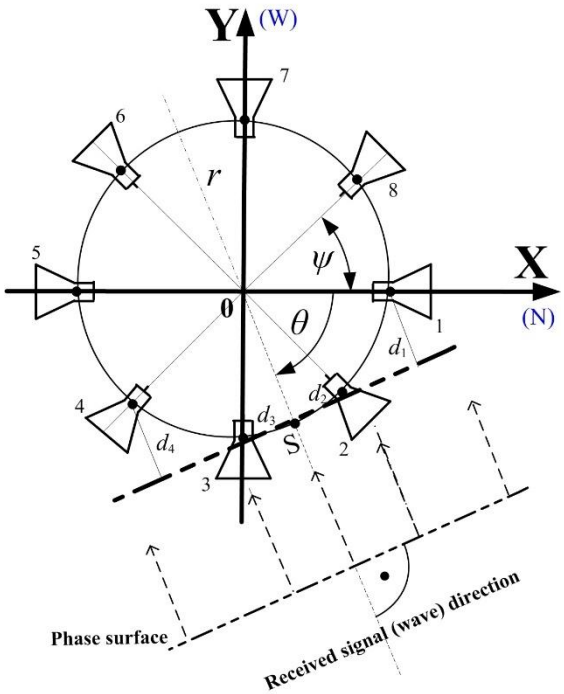

Figure 1. Antenna array in Cartesian coordinate system

For analytical description of the wave front in the adopted coordinate system, normal equation was used for the straight line tangent to the circle in *S* point. In this case, d_n distance of *n*-th antenna with x_n, y_n coordinates from the wave front is described by the following expression:

$$d_n = r\left|\cos\left[(n-1)\frac{2\pi}{N}\right]\cos(\theta)+\sin\left[(n-1)\frac{2\pi}{N}\right]\sin(\theta)-1\right| \quad (1)$$

The following expression describes A_n amplitude and the temporary phase φ_n of the signal at the output of *n*-th antenna:

$$A_n = \begin{cases} A_0 \dfrac{\sin\left(\frac{\pi}{\lambda} a_t \sin\left(\theta-(n-1)\frac{2\pi}{N}\right)\right)}{\frac{\pi}{\lambda} a_t \sin\left(\theta-(n-1)\frac{2\pi}{N}\right)} & \text{where } |\theta-\alpha_n| \le \frac{\pi}{2} \\ 0 & \text{where } |\theta-\alpha_n| > \frac{\pi}{2} \end{cases} \quad (2)$$

Analysis of aforementioned relationship reveals that the values of the signal amplitudes at the outputs of the respective antennas depend on the angle of the wave arrival, and signal phases depend on the radius of the circle of the analyzed antenna arrays, which is reflected in the relationship (1).

Based on relationship (2), the directivity characteristics of the respective antennas, which created the antenna array, were determined. Evaluation of influence of changes in level in the antenna characteristics crossing into the signal parameters occurring at their outputs was obtained by change in the width φ of the radiation characteristics. Figure 2. presents the directivity characteristics of the antenna elements, which are crossing at the levels of –2dB. Polar characteristics for second linear polarization is similarly presented in Figure 4.

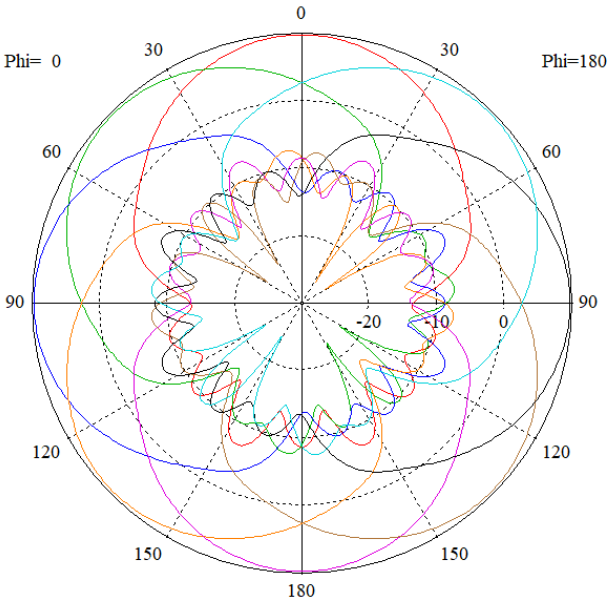

Figure 2. Polar directivity array elements characteristics

On the Cartesian characteristic, shown in Figure 3. and Figure 5., the intersection points of the directional characteristics of the elements of subsequent sectors were marked. These points are more than 2dB below the maximum gain level and, in angular terms, it is about ±23 deg and in relation to these angles in multiples of ±90 deg.

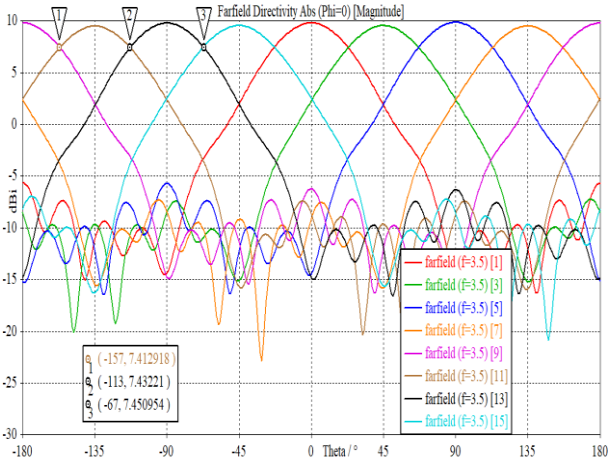

Figure 3. Cartesian elements directivity characteristics

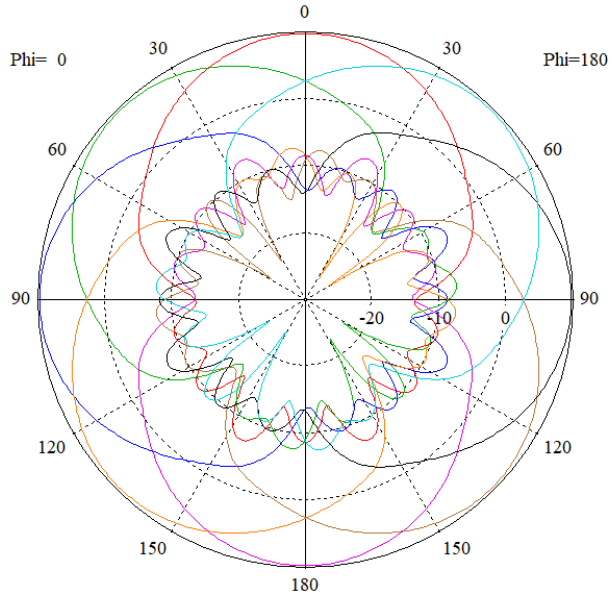

Figure 4. Polar characteristics second linear polarization

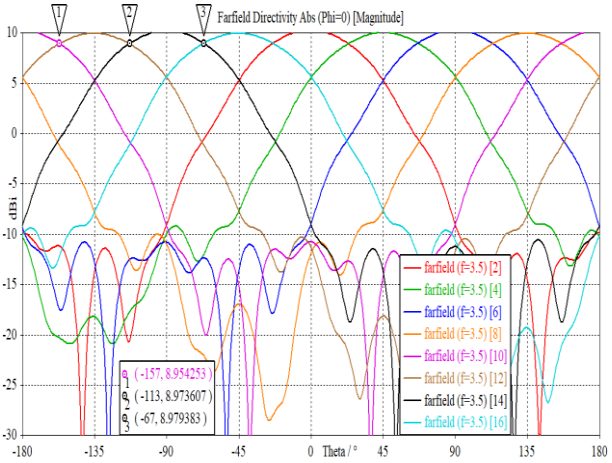

Figure 5. Cartesian elements directivity characteristics for second linear polarization

Figure 6. and Figure 7. present the directivity characteristics of the antenna array for both polarization in the polar and Cartesian systems respectively. Farfield characteristics for sector antenna array was shown in Figure 8. and it is quite similar to the characteristics of an omnidirectional antenna with gain 2.8dBi. The difference in gain level is approximately ±1dB.

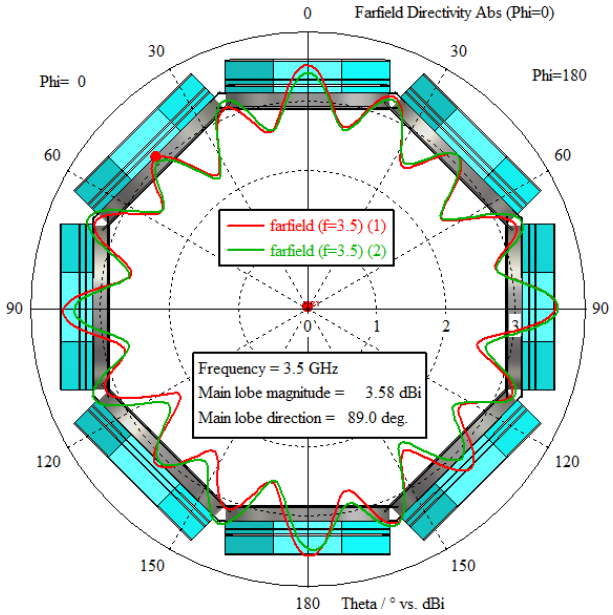

Figure 6. Polar directivity antenna array characteristics

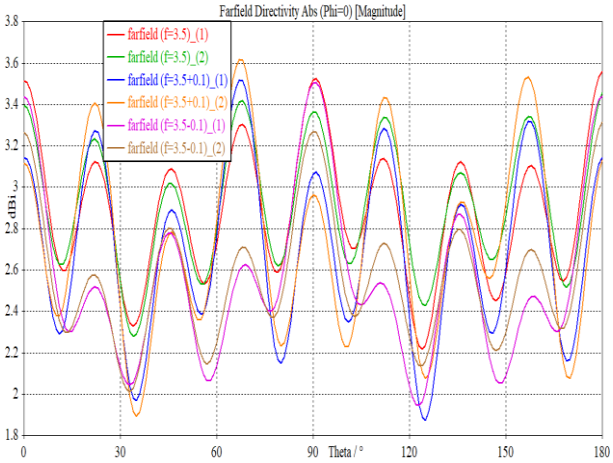

Figure 7. Cartesian array directivity characteristics

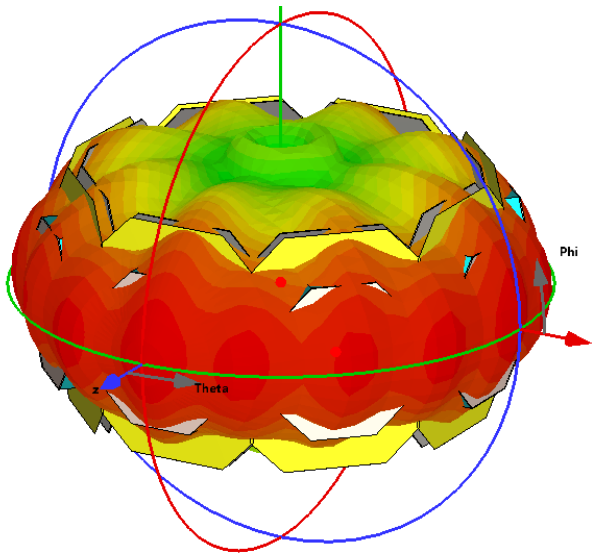

Figure 8. Multi-sector array farfield characteristics

The antenna array was built based on a modified element which farfield and gain characteristics are shown in Figure 9. and Figure 10. The changes included not only increasing the gain by 3 dB but also reducing the azimuth beamwidth to match the number of sectors. For example, 90 degrees for 6 sectors and

about 60 degrees for 8 sectors. The beamwidth can be controlled by connecting elements, but this requires increasing their number by two or more. The bandwidth of each element has also been increased to 700MHz. The antenna element parameters are summarized in Table 1.

In order to reduce the number of elements, circular polarization was obtained from each element so that it was not necessary to connect the elements with phase shifting shown in Figure 11. The parameters of the connected elements are shown in Figure 12. The gain characteristics of a single element and a combination of four are shown in the Figure 10. and Figure 13, respectively. Circular polarization was obtained in one element by exciting signals both linear polarizations.

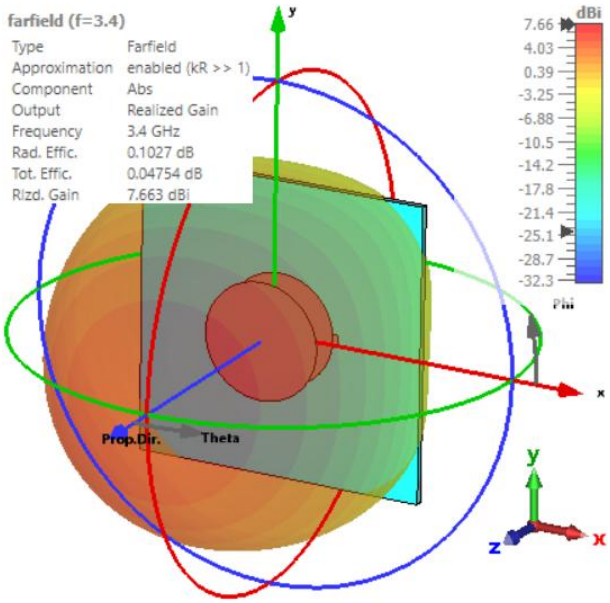

Figure 9. Antenna element farfield characteristic

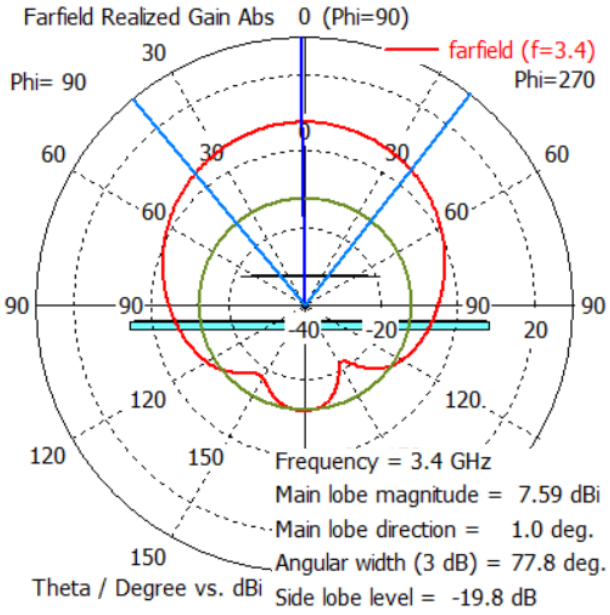

Figure 10. Polar gain characteristic of antenna element

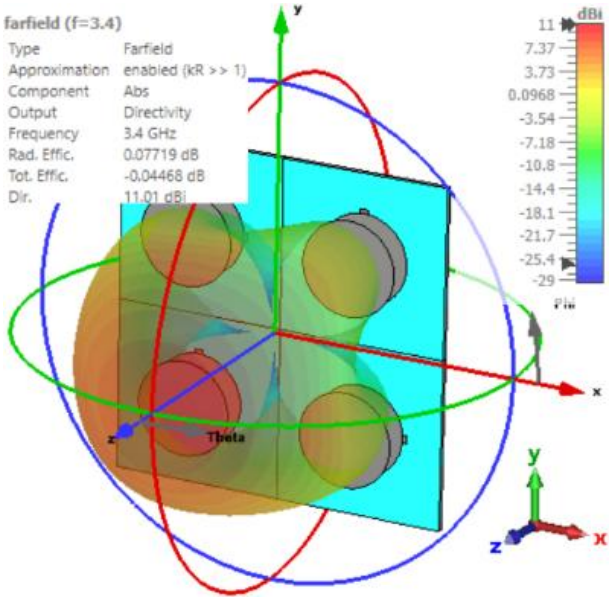

Figure 11. 4 elements antenna farfield characteristic

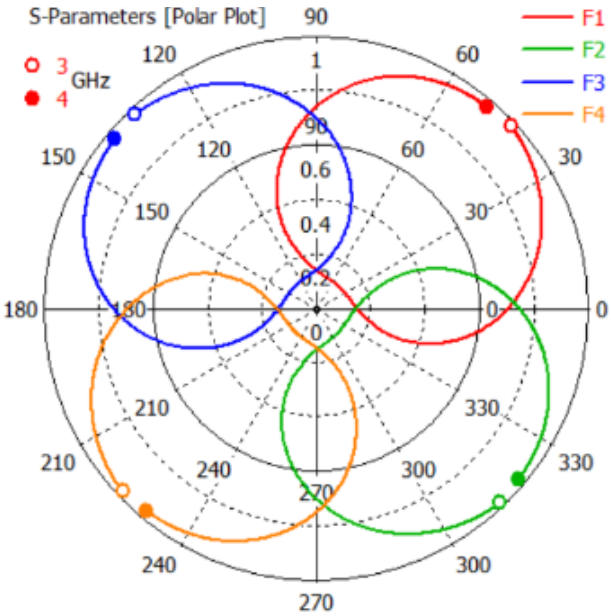

Figure 12. S-parameters characteristics of elements

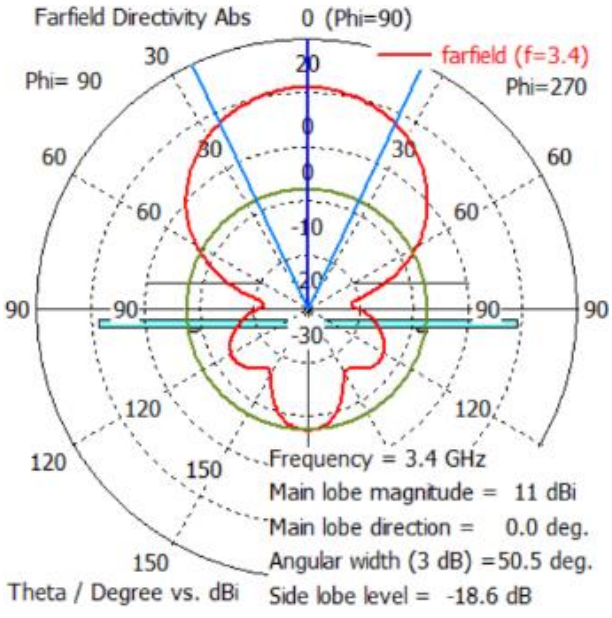

Figure 13. Polar gain characteristic of 4 antenna elements

Table 1. The modified antenna element parameters

Parameter		Value	Unit
"Antenna element gain"		9.8	dBi
SLL		>-15	dB
"f" _"C"		3.5	GHz
WFS		<1.5	[--]
"Bandwidth"		>700	MHz
"3dB Beamwidth"	Vertical	59	°
"3dB Beamwidth"	Horizontal	360	°

Figure 14. presents the directivity of antenna sector, consisting of 3 elements in column, depending on the angle in elevation. For comparison, the Figure 16. shows directivity for 7 elements in column. As expected, it is possible to achieve larger angles up to ±45 degrees for 7 elements for not worse SLL levels in this case >26dB. In practice, a better solution will be to make two columns of 3 elements, one above the other, set at a e.g. 60 deg. angle.

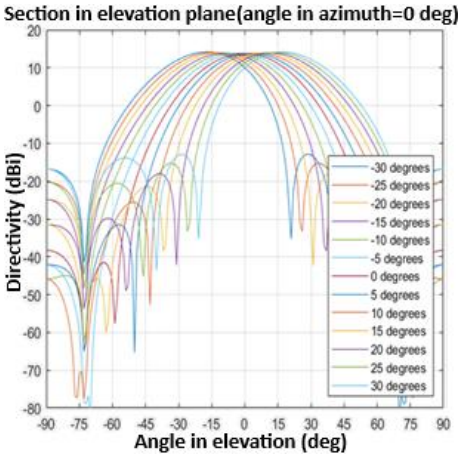

Figure 14. Directivity characteristic 3 elements column

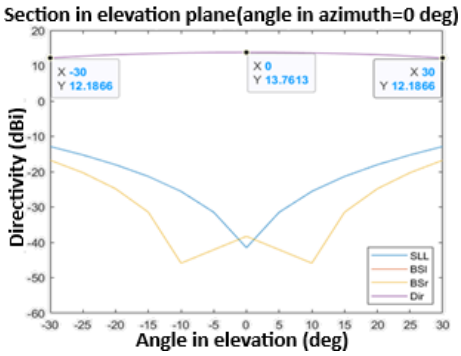

Figure 15. Parameters characteristics of 3 elements array

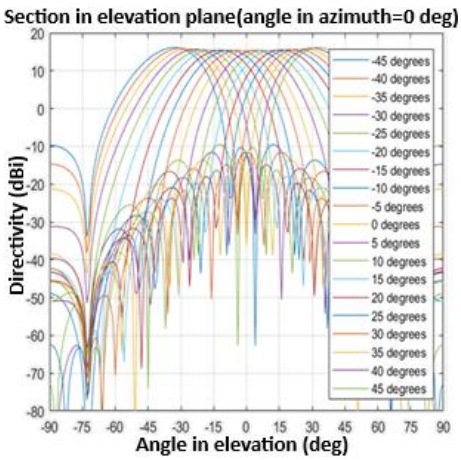

Figure 16. Directivity characteristic 7 elements column

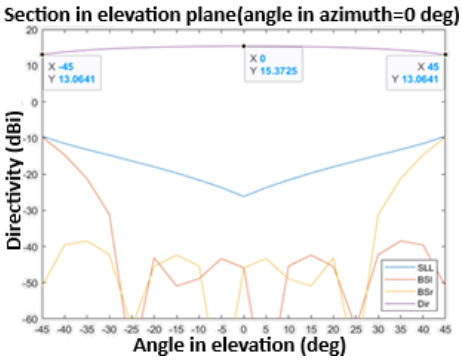

Figure 17. Parameters characteristics of 7 elements array

Figure 15. and Figure 17. show not only the directivity characteristics depending on the angle but also the side lobe level SLL for 3 and 7 antenna elements in a column (array) respectively. calculations were performed for 0.5λ and 0.4λ spacings and other parameters contained in the Table 1. The characteristics show that the practical SLL level that can be achieved is 20 dB in the entire angular range of ±30 degrees for 3 elements in a column and in the range of ±45 degrees for 7 elements. Regardless of the number of elements, the best parameters are obtained in the angular range of ±30 degrees, therefore, illuminating with additional elements is a more effective solution compared to a larger number of elements in the column.

Figure 18. shows the structure of the model of the selected sector. In order to obtain a gain of approximately 10dBi from each element, lenses can be used due to the sharing of a screen by all elements limiting directivity the connected radiators constitute the central element of the column. Connecting the middle elements allows to reduce the distance between the electrical centers below 0.5λ for elements whose dimensions prevent closer proximity in order to reduce the SLL to the minimum possible levels.

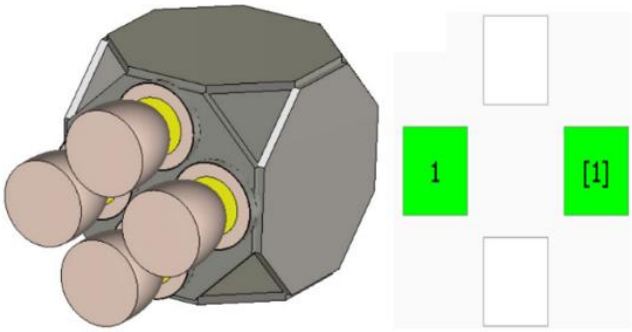

Figure 18. Antenna array 2x2 with and without holder

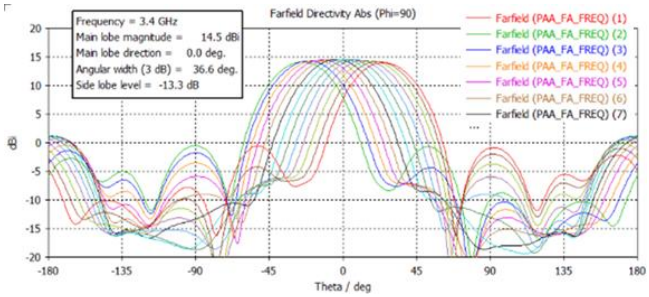

Figure 19. Antenna array 2x2 directivity without holder

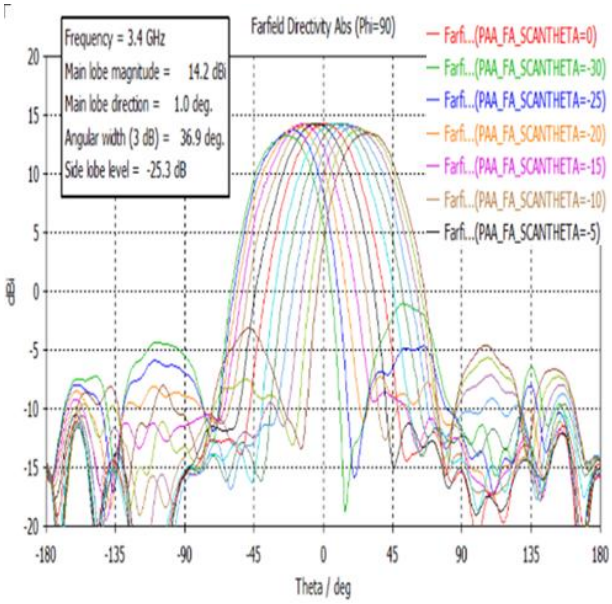

Figure 20. Antenna array 2x2 directivity with holder

The directional characteristics are shown in Figure 19. and Figure 20., respectively, without and with the model housing and as expected, the level of back radiation is lower with antenna array mounting. The obtained SLL level of >-15dB can be improved by increasing the gain of the antenna element to about 12dBi, but this will require increasing the number of sectors to 12. Practical SLL levels that can be achieved are from 17dB to 20dB.

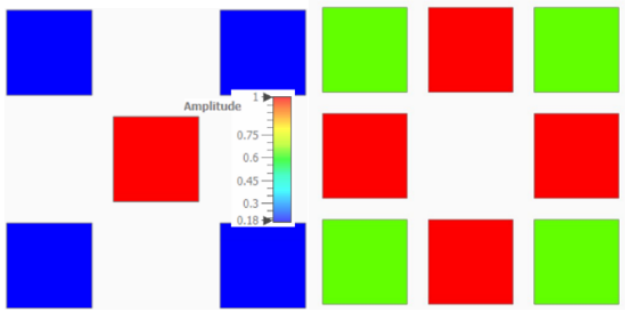

Figure 21. Arrays 2x1x2 and 3x2x3 amplitude tapering

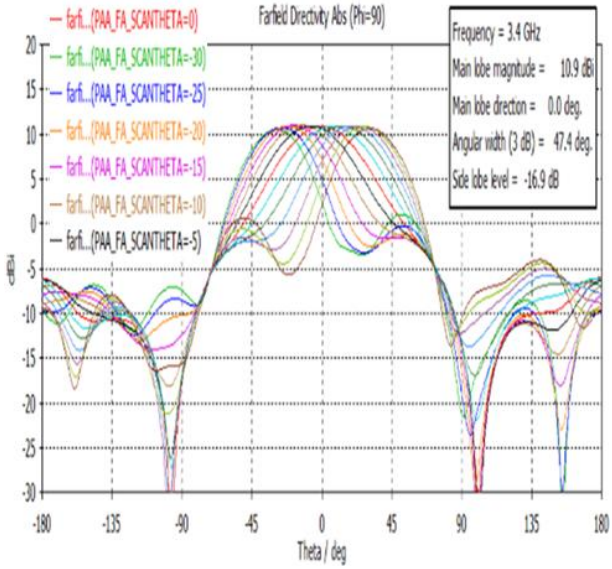

Figure 22. Array 2x1x2 directivity in angle range

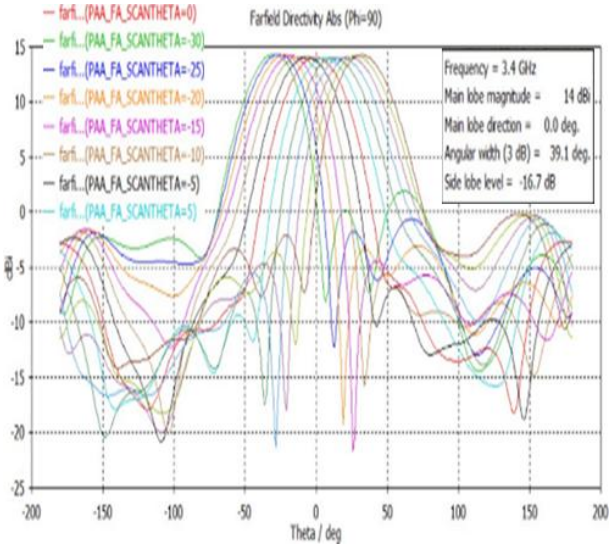

Figure 23. Array 3x2x3 directivity in angle range

Figure 21. shows the model structure of connecting adjacent sectors for a maximum of 3 rows and various arrangements. The directional characteristics of arrays 2x1x2 and 3x2x3 are shown in Figure 22. and Figure 23., respectively. The advantage of the 3x2x3 arrangement is the equalization of directivity levels for the entire angular range but this comes at the cost of a higher level of side lobes at maximum angles. Skillful arrangement of element connections and tapering are key for optimization.

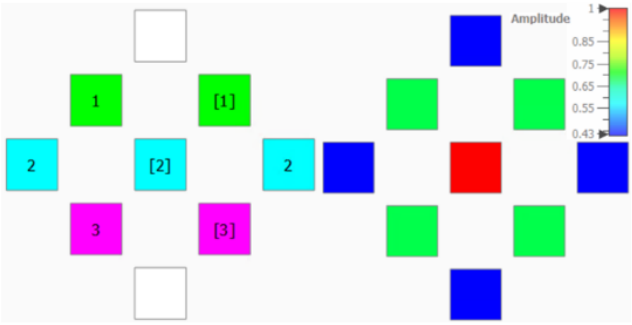

Figure 24. Antenna array 3x3 amplitude tapering

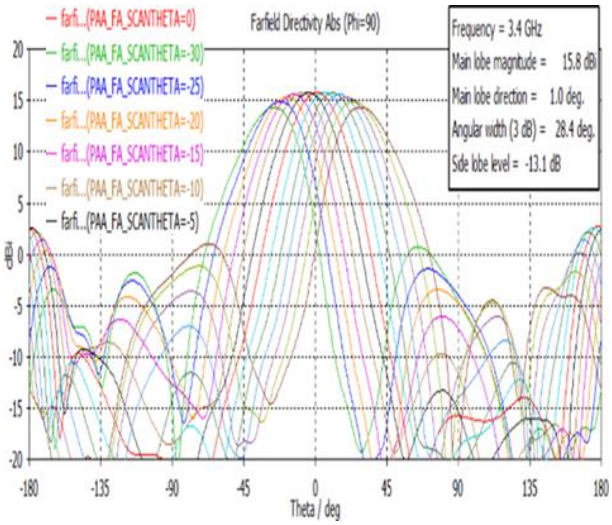

Figure 25. Antenna array 3x3 directivity, Phi=90

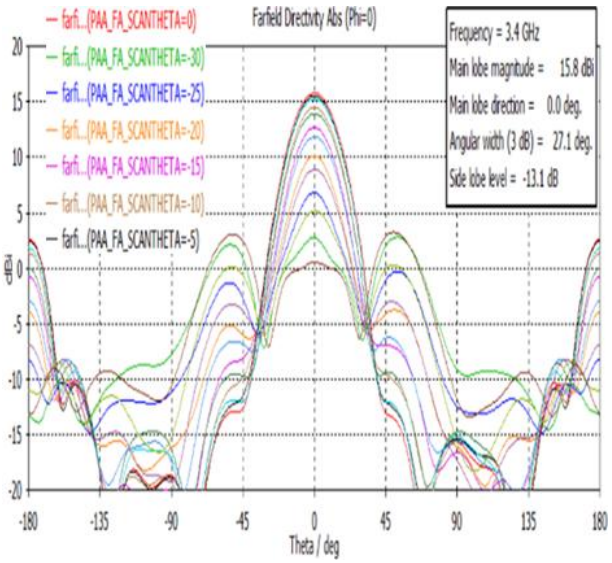

Figure 26. Antenna array 3x3 directivity, Phi=0

Figure 24. shows the model structure of connecting adjacent sectors in the case of a larger number of rows in the presented example of 5. The directional characteristics of array 3x3x3 are shown in Figure 25. and Figure 26. Apart from increasing gain, there are no noticeable benefits in such an arrangement. The SLL levels are slightly lower for larger angles. A more effective solution is to use additional elements to illuminate the maximum angles, not simultaneously +30deg or -30deg. This allows effectively combine a column of maximum four elements.

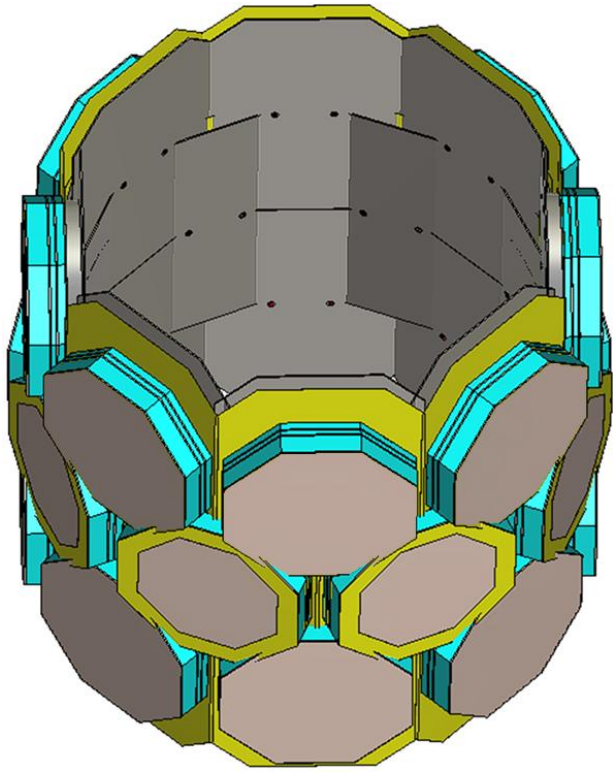

Figure 27. Three-row modified cylindrical antenna array

Based on the presented elements and antenna arrays the model shown in Figure 27. was also designed in addition to the model with one element in the column. It is possible to control beams in columns or rows of the array. Skillful element combinations allow to achieve gain close to 20dBi level while maintaining low sidelobe levels of 15dBc to 20dBc. The small number of elements limits beam steering to an angular range of ±30 degrees in elevation. Gain adjustments are made by selecting the power levels of the control signals.

Arranging elements in a zigzag pattern allows you to double the number of columns but forces to reduce the width of the beam from a single element. Changing the beam width is also beneficial due to reducing the level of coupling between elements. Due to the limited space, greater gain can be achieved by using horns or planar antennas with lenses. Further work will concern the analysis of the feasibility of prototype mechanics, not only with overlapping elements but also with conformal ones. The power levels of the stimulating signals will also be optimized.

3 CONCLUSIONS

Radiation characteristics of cylindrical antenna array elements were calculated. A system of 8 elements with one for each sector based on patch antennas was designed. Electromagnetic simulations were performed, which resulted in obtaining radiation characteristics of the antenna array operating in the S-band, consistent with the calculations performed. The simulations with 3 and more elements in the array columns were performed not only to increase the gain of the antenna array but also to be able to control the beam angle in each sector independently.

REFERENCES

[1] J. Stępień, "Localization Methods in MF and UHF Reserve Radionavigation System", NTSP, 2020.
[2] J. Stępień, "Review of S-band and X-band Antennas and Filters for both Maritime and Space applications", ISAP, 2021.
[3] D. Zmysłowski, P. Skokowski, K. Malon, K. Maślanka, J.M. Kelner, "Naval Use Cases of 5G Technology", 09 2023, TransNav 17(3):595-603.
[4] D. Zmysłowski, K. Kryk, J.M. Kelner, "Testing GNSS receiver robustness for jamming" December 2023 "Aviation and Security Issues" 4(2):139–155.
[5] NTT DOCOMO, INC., "5G Evolution and 6G", White Paper, Version 5.0, 01/2023.
[6] Go Otsuru, Hiroyuki Tsuji, Ryu Miura, Jun Suzuki, Yoshihisa Kishiyama, "Efficient Antenna Tracking Algorithm for HAPS Ground Station in Millimeter-Wave", WPMC, 2022.
[7] Cezary Ziółkowski; Jan M. Kelner, "Angular Separation of Channels in 5G System Multi-Beam Antennas", ICMCIS, 2019.
[8] Jan M. Kelner; Cezary Ziółkowski, "Spatial Multiplexing of Channels by Using Multi-beam Antenna System for 60 GHz", PIERS, 2019.
[9] Kamil Bechta; Jinfeng Du; Marcin Rybakowski, "Optimized Antenna Array for Improving Performance of 5G mmWave Fixed Wireless Access in Suburban Environment", 5GWF, 2019.
[10] Jan M. Kelner and Cezary Ziółkowski, "Interference in Multi-beam Antenna System of 5G Network", IJET, 2020.
[11] Kamil Bechta, Cezary Ziółkowski, Jan M. Kelner and Leszek Nowosielski, "Modeling of Downlink Interference in Massive MIMO 5G Macro-Cell", MDPI Sensors, 2021.
[12] Kamil Bechta, Jan M. Kelner, Cezary Ziółkowski and Leszek Nowosielski, "Inter-Beam Co-Channel Downlink and Uplink Interference for 5G New Radio in mm-Wave Bands", MDPI Sensors, 2021.

[13] Jarosław Wojtuń,Cezary Ziółkowski and Jan M. Kelner, "Modification of Simple Antenna Pattern Models for Inter-Beam Interference Assessment in Massive Multiple-Input–Multiple-Output Systems", MDPI Sensors, 2023.
[14] Cezary Ziółkowski, Jan M. Kelner, "Antenna pattern in three-dimensional modelling of the arrival angle in simulation studies of wireless channels", IET, 2017.
[15] Cezary Ziółkowski; Jan M. Kelner, "Statistical Evaluation of the Azimuth and Elevation Angles Seen at the Output of the Receiving Antenna", IEEE Transactions on Antennas and Propagation, 2018.
[16] ETSI TR 138 901 V18.0.0, "5G; Study on channel model for frequencies from 0.5 to 100 GHz", 2024.